The day/night switch in KaiC, a central oscillator component of the circadian clock of cyanobacteria

Yong-Ick Kim*, Guogang Dong[†‡], Carl W. Carruthers, Jr.*, Susan S. Golden[†‡], and Andy LiWang[§¶]

*Department of Biochemistry and Biophysics, Texas A&M University, College Station, TX 77843-2128; [†]Center for Research on Biological Clocks, Texas A&M University, College Station, TX 77843; [‡]Department of Biology, Texas A&M University, College Station, TX 77843-3258; and [§]School of Natural Sciences, University of California at Merced, 4225 North Hospital Road, Atwater, CA 95301

Edited by Joseph S. Takahashi, Northwestern University, Evanston, IL, and approved June 25, 2008 (received for review January 18, 2008)

The circadian oscillator of the cyanobacterium *Synechococcus elongatus* is composed of only three proteins, KaiA, KaiB, and KaiC, which, together with ATP, can generate a self-sustained ≈24 h oscillation of KaiC phosphorylation for several days. KaiA induces KaiC to autophosphorylate, whereas KaiB blocks the stimulation of KaiC by KaiA, which allows KaiC to autodephosphorylate. We propose and support a model in which the C-terminal loops of KaiC, the ''A-loops'', are the master switch that determines overall KaiC activity. When the A-loops are in their buried state, KaiC is an autophosphatase. When the A-loops are exposed, however, KaiC is an autokinase. A dynamic equilibrium likely exists between the buried and exposed states, which determines the steady-state level of phosphorylation of KaiC. The data suggest that KaiA stabilizes the exposed state of the A-loops through direct binding. We also show evidence that if KaiA cannot stabilize the exposed state, KaiC remains hypophosphorylated. We propose that KaiB inactivates KaiA by preventing it from stabilizing the exposed state of the A-loops. Thus, KaiA and KaiB likely act by shifting the dynamic equilibrium of the A-loops between exposed and buried states, which shifts the balance of autokinase and autophosphatase activities of KaiC. A-loop exposure likely moves the ATP closer to the sites of phosphorylation, and we show evidence in support of how this movement may be accomplished.

kinase | phosphatase | phosphorylation | NMR | X-ray

Virtually all light-perceiving organisms display circadian (≈24-h) rhythms in their gene activity, metabolism, physiology, and behavior in anticipation of and preparation for daily swings in sunlight and ambient temperature (1, 2). These robust biological rhythms are the result of an endogenous clock called the circadian clock and have been identified in cyanobacteria (3, 4). In the cyanobacterium *Synechococcus elongatus*, the clock is important for reproductive fitness (5, 6), and expression of the entire genome is under clock control (7, 8).

Only three proteins make up the central oscillator of the *S. elongatus* clock (9): KaiA, KaiB, and KaiC. The high-resolution structures of all three proteins are known (10–15). Remarkably, the central oscillator can be reconstituted in a test tube (16). A simple mixture of the three proteins and ATP regenerates the sustained cellular ≈24-h rhythm of KaiC phosphorylation. Temperature compensation and mutant rhythm phenotypes observed *in vivo* are also reproduced by this clock-in-a-test tube.

An ensemble of KaiC molecules exhibits both autokinase and autophosphatase activities (10, 17, 18). In *S. elongatus*, the balance between these two activities swings back and forth on a daily basis. *In vivo*, KaiC is hyperphosphorylated during the night and hypophosphorylated during the day (19, 20). There are two phosphorylation sites on KaiC, S431 and T432 (21, 22). The distribution of KaiC phosphoforms over a ≈24 h period proceeds as ST-KaiC (unphosphorylated) → SpT-KaiC (T432 phosphorylated) → pSpT-KaiC (S431 and T432 phosphorylated) → pST-KaiC (S431 phosphorylated) → ST-KaiC (23, 24), although individual KaiC molecules do not necessarily go all of the way around the loop (24). Alone, the autophosphatase activity of KaiC is dominant; KaiA shifts the balance of activities from autophosphatase to autokinase (10, 17, 19). However, the pST-KaiC phosphoform recruits KaiB, and, together, they inactivate KaiA in KaiABC complexes (23–25). With insufficient levels of active KaiA in solution, the ensemble of KaiC molecules begins to dephosphorylate. KaiA activity resumes once enough pST-KaiC has decayed to ST-KaiC [implying that not all KaiC molecules make it back to the ST-KaiC state before being restimulated by KaiA to autophosphorylate (24)]. Monomer shuffling between KaiC hexamers may play a role in synchronization (26, 27).

The phosphorylation cycle of KaiC is apparently integrated with a transcription/translation oscillator (28) to maintain stable 24-h cellular rhythms in *S. elongatus* genes (7, 8). Thus, it is of central importance to understand how KaiA and KaiB shift the relative autokinase and autophosphatase rates in KaiC. Here, we present evidence that a segment of residues near the C terminus of each KaiC subunit determines which activity is dominant. We propose that when these ''A-loops'' are buried, KaiC is an autophosphatase. However, when the A-loops are exposed, KaiC is an autokinase. We suggest that there is a dynamic equilibrium between the buried and exposed states of the A-loops, so that an ensemble of KaiC molecules exhibits both activities simultaneously. In the absence of other proteins, KaiC is both an autokinase and autophosphatase, with the latter activity dominant over the former (10, 17, 19). In this case, according to our model the dynamic equilibrium favors the buried state of the A-loops. We propose that KaiA stabilizes the exposed state, thereby increasing the autokinase rate relative to that of the autophosphatase. We think that KaiB acts by preventing this KaiA-mediated stabilization.

Results

The Equilibrium Position of the A-Loop Determines the Steady-State Phosphorylation Level of KaiC. Shown in Fig. 1*A* is the NMR structure of the complex between the C-terminal domain of KaiA, KaiA^{C}, and a peptide derived from C-terminal residues 488–518 of KaiC, both from *Thermosynechococcus elongatus* (29). The x-ray crystal structure of *S. elongatus* KaiC (Fig. 1*B*) shows that residues 488–497 (magenta) are buried in a looped conformation (15). Here, we refer to this stretch of residues as the A-loop. ''Tail'' residues 498–519 are not resolved in this x-ray crystal structure but are seen to protrude from the top of KaiC in a later study (30). The homologous solvent-exposed tail residues from *T. elongatus* are colored yellow in Fig. 1*A*. The

Author contributions: Y.-I.K., G.D., C.W.C., S.S.G., and A.L. designed research; Y.-I.K., G.D., and C.W.C. performed research; Y.-I.K., G.D., C.W.C., S.S.G., and A.L. analyzed data; and Y.-I.K., G.D., S.S.G., and A.L. wrote the paper.

The authors declare no conflict of interest.

This article is a PNAS Direct Submission.

¶To whom correspondence should be addressed. E-mail: aliwang@ucmerced.edu.

This article contains supporting information online at www.pnas.org/cgi/content/full/0800526105/DCSupplemental.

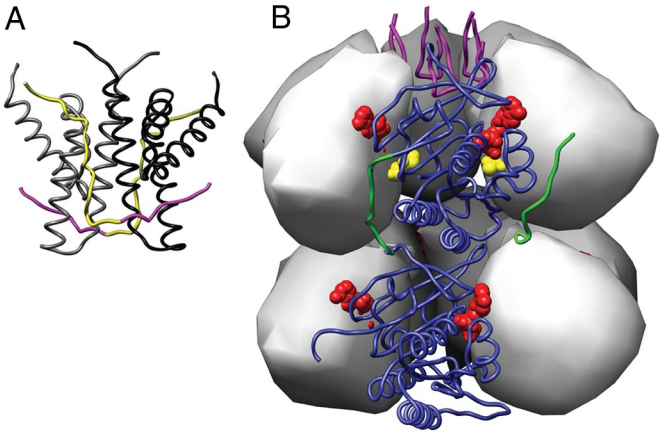

Fig. 1. The NMR structure of the *T. elongatus* KaiA^{C}– KaiC$^{AL+tail}$ complex (*A*) and x-ray crystal structure of KaiC from *S. elongatus* (*B*). (*A*) The two subunits of the KaiA^{C} dimer of the KaiA^{C}–KaiC$^{AL+tail}$ complex (PDB ID code 1suy) are shown as black and gray ribbons. The two bound KaiC$^{AL+tail}$ peptides are shown as ribbons, with the A-loop segment colored magenta and the tail segment colored yellow. (*B*) The N- and C-terminal domains of five subunits of KaiC (PDB ID code 1tf7) are shown as gray surfaces, whereas those of the remaining subunit are shown as a blue ribbon. The polypeptide segment connecting the two domains is shown as a green ribbon. The A-loops are shown as magenta ribbons. The solvent-exposed C-terminal residues 498–519 are unresolved in this structure. ATP molecules are red and S431 and T432 are yellow. All figures of Kai protein structures were created using the program Chimera (40).

A-loop + tail segment of KaiC (KaiC$^{AL+tail}$) from *S. elongatus* and *T. elongatus* are 61% identical and 84% similar. In addition, residues in *T. elongatus* KaiA^{C} that interact with KaiC$^{AL+tail}$ according to the NMR structure share a high level of identity with *S. elongatus* KaiA^{C} (29). In the present study, all experiments were performed using *S. elongatus* proteins, except for one set of fluorescence anisotropy experiments (Fig. 4*B*).

A comparison of Fig. 1 *A* and *B* suggested that A-loops have two states, buried as seen in Fig. 1*B* and exposed as implied by Fig. 1*A*. In our model, the A-loops in an ensemble of KaiC molecules exist in a dynamic equilibrium between buried and exposed states, which determines the steady-state level of phosphorylation of KaiC. If the equilibrium favored the buried state, the rate of autodephosphorylation would have been faster than that of autophosphorylation. In contrast, if the exposed state were favored, then the autokinase rate would be faster, leading to a high steady-state phosphorylation level for KaiC. According to our model, KaiA increased KaiC phosphorylation levels by stabilizing the exposed state of the A-loops by directly binding to KaiC$^{AL+tail}$.

As a test of our model, we made a variant of KaiC to mimic the exposed state of A-loops. This variant, KaiC487, was truncated after residue 487 and, therefore, missing the KaiC$^{AL+tail}$ segment. As seen in Fig. 2*A* (green ○), KaiC487 by itself was constitutively 100% phosphorylated. A recent study has shown that the steady-state phosphorylation level for *S. elongatus* KaiC under increasing concentrations of KaiA does not exceed ≈85% (31). Another study has shown, for *T. elongatus* proteins, that a ratio of one KaiA dimer to one KaiC hexamer is enough to reach saturation level of phosphorylation, which is also <100% (32). KaiA cannot induce 100% phosphorylation of a population of KaiC molecules because, even under saturating conditions, A-loops probably still sample the buried state to a minor extent.

Our model predicted that reducing the ability of KaiA to stabilize the exposed state of the A-loops should lead to a lower steady-state level of KaiC phosphorylation. We, therefore, produced a KaiC variant, KaiC497, which was truncated after

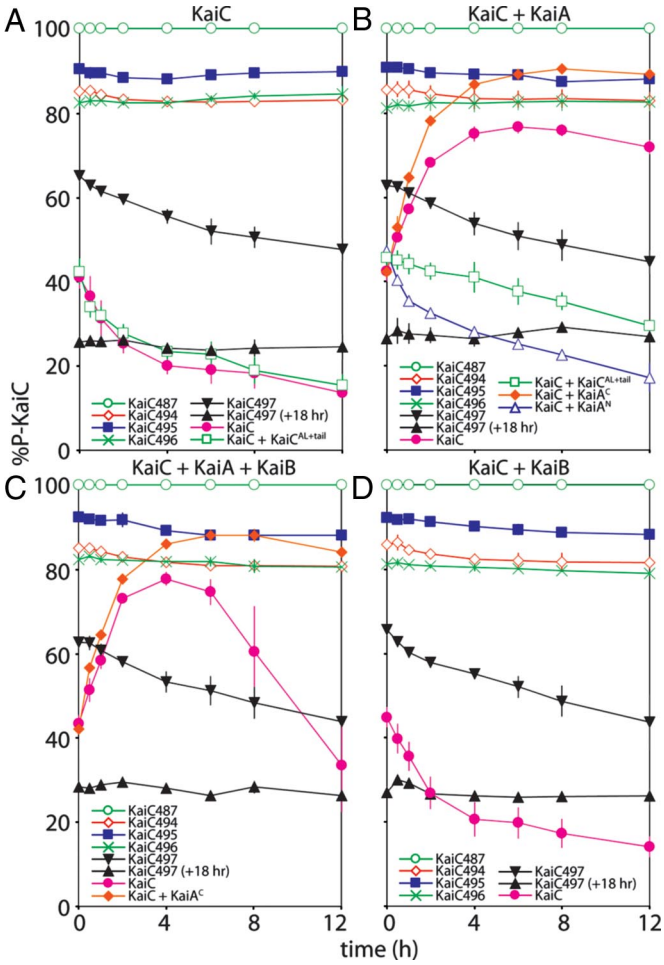

Fig. 2. Phosphorylation of KaiC and KaiC variants for KaiC alone (*A*), KaiC + KaiA (*B*), KaiC + KaiA + KaiB (*C*), and KaiC + KaiB (*D*). For all images: pink ●, KaiC; black ▼ and ▲, KaiC497; green ×, KaiC496; blue ■, KaiC495; red ◇, KaiC494; green ○, KaiC487. In *A*, green □ indicates KaiC + KaiC$^{AL+tail}$ (500 μM). In *B*, green □ indicates KaiC + KaiC$^{AL+tail}$ (500 μM) + KaiA; blue △, KaiC + KaiA^{N} only; and orange ◆, KaiC + KaiA^{C} only. In *C*, orange ◆ indicates KaiC + KaiA^{C} + KaiB. Each data point is the mean of two independent experiments. Solid lines connect data points for visual clarity. Images of the stained polyacrylamide gels are shown in supporting information (SI) Fig. S1. Assignment of phosphorylated and unphosphorylated KaiC bands resolved by PAGE was determined from lambda phosphatase assays (Fig. S2). All KaiC samples were fresh or from freshly frozen samples except for data indicated by black ▲ symbols, which are from KaiC497 reaction mixtures after incubation at 30°C for 18 h ± KaiA ± KaiB. It should be noted that the phosphorylation levels of KaiC487, KaiC494, KaiC495, and KaiC496 after incubation at 30°C for 18 h ± KaiA ± KaiB remained similar to those after the initial 12 h (data not shown).

residue 497, so that it had the A-loop but was missing the solvent-exposed tail. The steady-state phosphorylation levels of KaiC497 alone and in the presence of KaiA were similarly low (Fig. 2 *A* and *B*, black ▼ and ▲), which suggests that the dynamic equilibrium of the A-loop in both cases is shifted toward the buried state. A KaiC variant similar to KaiC497 is unable to form a complex with KaiA, as determined by electrophoretic mobility-shift assays (30). Truncations partway into the A-loop resulted in KaiC variants that were hyperphosphorylated (Fig. 2*A*, green ×, blue ■, and red ◇), although to a lesser extent than KaiC487 (green ○). To a minor extent, these truncated A-loops may still sample the buried state, thus leading to <100% steady-state phosphorylation levels. In addition to deletion experiments, KaiC variants containing point mutations in or bordering the A-loop were also made to test our model. In the structure of

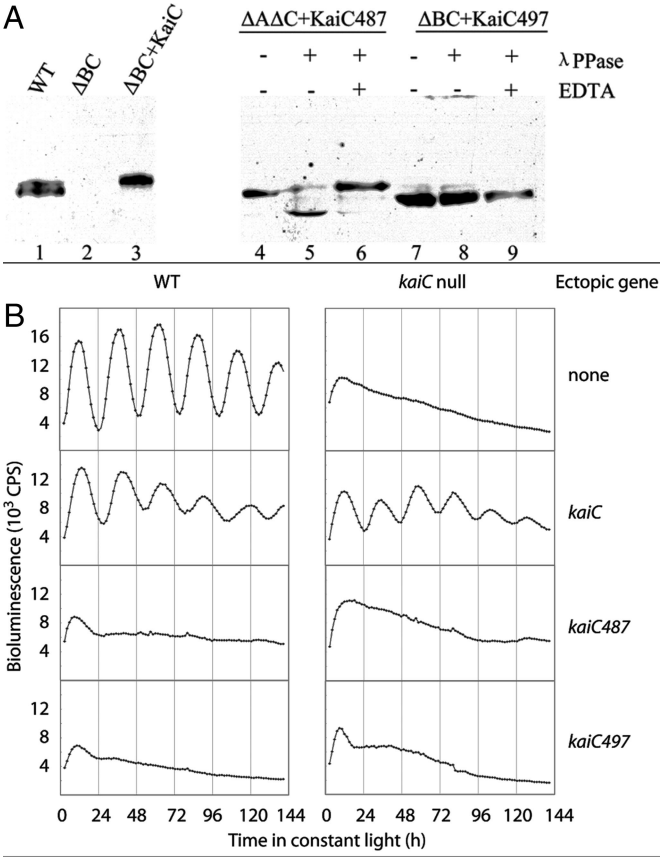

Fig. 3. Phosphorylation states and functional analysis of KaiC487 and KaiC497 *in vivo*. (*A*) KaiC487 and KaiC497 are, respectively, constitutively hyper- and hypophosphorylated independently of KaiA in *S. elongatus*. Immunoblots of KaiC and its truncated variants were detected in soluble protein extracts from strains that express: lane 1, WT KaiC; lane 2, no KaiB or KaiC; lane 3, WT KaiC from an ectopic site in a *kaiBC* null background (KaiA is present); lanes 4–6, KaiC487 from an ectopic site in a *kaiA kaiC*-null background (KaiB is present); lanes 7–9, KaiC497 in a *kaiBC*-null background (KaiA is present). The phosphorylation status of KaiC variants, whose mobility differs from WT was determined by λ phosphatase treatment with (lanes 6 and 9) or without (lanes 5 and 8) the inhibitor EDTA. Total cell extracts from 10 ml of $OD_{750} = 0.5$ cyanobacterial cultures were prepared and further analyzed by immunoblotting (41) with polyclonal KaiC antiserum (42) at 1:2,000 dilution. Treatment with λ phosphatase was performed according to the recommendation of the manufacture (New England BioLabs). Briefly, 100 μg of total protein was incubated with 400 units of λ phosphatase in 50 μl of total volume at 30°C for 30 min. EDTA was used at a final concentration of 50 mM to inhibit the phosphatase reaction. (*B*) Ectopic expression of KaiC487 or KaiC497 abolishes circadian rhythmicity in WT *S. elongatus*. WT KaiC, KaiC487, and KaiC497 are expressed from the native *kaiBC* promoter in a WT (*Left*) or *kaiC* null (*Right*) background. All strains harbor a bioluminescence reporter gene driven by the *kaiBC* promoter.

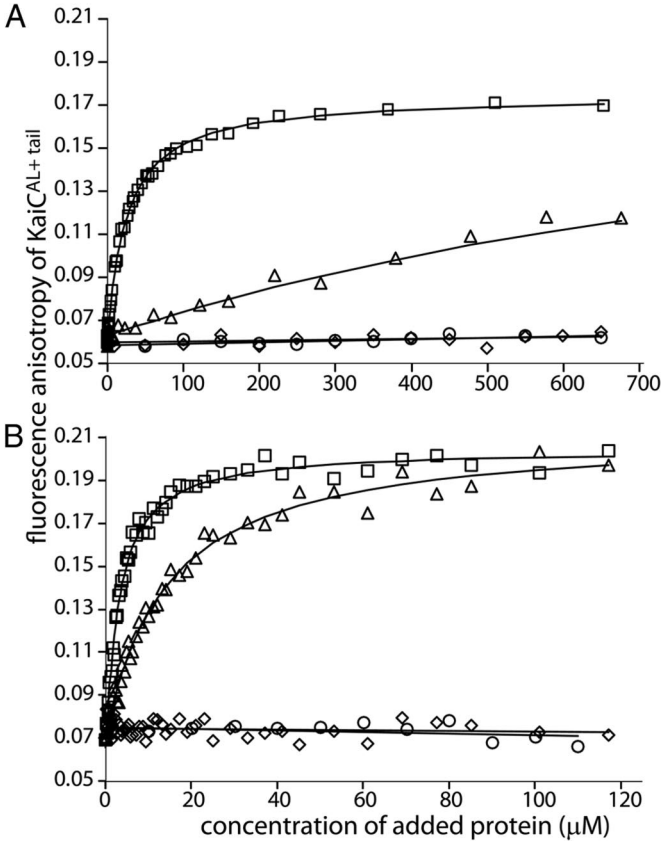

Fig. 4. Fluorescence anisotropy of 6-iodoacetamidofluorescein-KaiC$^{AL+tail}$ as a function of concentration of KaiA for *S. elongatus* (*A*) and *T. elongatus* (*B*) proteins. △ indicates KaiA; □, KaiA^{C}; ◇, KaiA^{N}; and ○, KaiB. Fits of the data yielded the following K_d values: 24.3 ± 0.5 μM, *S. elongatus* KaiA^{C} + KaiC$^{AL+tail}$; 170 ± 13 μM, *S. elongatus* KaiA + KaiC$^{AL+tail}$; 2.9 ± 0.2 μM, *T. elongatus* KaiA^{C} + KaiC$^{AL+tail}$; 14.4 ± 1.1 μM, *T. elongatus* KaiA + KaiC$^{AL+tail}$.

KaiC, the side chains of residues E487 and T495 appeared to be hydrogen-bonded to each other (Fig. S3), suggesting that the buried state of the A-loop was stabilized by this interaction. Indeed, the E487A substitution created a KaiC variant that was 100% constitutively phosphorylated, whereas the T495A variant was 80% constitutively phosphorylated (Fig. S4).

KaiC487 and KaiC497 expressed in *S. elongatus* were, respectively, hyper- and hypophosphorylated as well (Fig. 3*A*); moreover, KaiC487 remained hyperphosphorylated even when KaiA was absent and KaiB was present (Fig. 3*A*, lanes 4–6), and KaiC497 remained hypophosphorylated when KaiA was present and KaiB was absent (lanes 7–9). In addition, ectopic expression of either KaiC487 or KaiC497 in a WT *S. elongatus* background had a dominant negative effect, abolishing circadian rhythmicity (Fig. 3*B*), even though they had opposite states of phosphorylation. In contrast, rhythmicity was preserved when WT KaiC was expressed in a WT background, with a slightly longer free-running period than normal (Fig. 3*B* and Fig. S5).

KaiC497 and KaiC496, which differ only in the presence or absence of I497, had opposite steady-state levels of phosphorylation (Fig. 2*A*, black ▲ and green ×). This result suggests that I497, the terminal residue of the A-loop, plays a critical role in stabilizing the buried position of the A-loop. It can be seen from the structure of KaiC (Fig. S6) that I497 is apparently part of an intrasubunit hydrophobic cluster that includes residues V443, I445, I467, F483, F486, I489, I490, P494, and T495. Perhaps the removal of I497 in KaiC496 was sufficient to destabilize the cluster and thereby shift the dynamic equilibrium of the A-loop toward the exposed state.

KaiA Activates KaiC Autophosphorylation by Directly Binding to the A-Loop + Exposed Tail Segment. The structure of the KaiA^{C}–KaiC$^{AL+tail}$ complex has been solved for the polypeptides from the thermophilic species *T. elongatus*, which are more stable under NMR conditions (Fig. 1*A*) (29). To test whether this interaction is similar for the *S. elongatus* homologs, we carried out fluorescence anisotropy assays. The fluorescence anisotropy of a fluorophore is sensitive to the size of the macromolecule to which it is attached. An increase in the fluorescence anisotropy of a labeled peptide after the addition of unlabeled protein can reflect the formation of complexes. As seen in Fig. 4*A*, *S.*

elongatus KaiA and KaiC$^{AL+tail}$ interacted, although to a weaker extent than for the *T. elongatus* proteins (Fig. 4*B*). As a further test of the KaiA–KaiC$^{AL+tail}$ interaction, we added *S. elongatus* KaiC$^{AL+tail}$ peptides to a mixture of *S. elongatus* KaiA + KaiC. As shown by the green □ symbols in Fig. 2*B*, KaiC$^{AL+tail}$ blocked KaiA-induced KaiC autophosphorylation, which suggests that this peptide was competing with KaiC for KaiA binding. The K_D values observed here were much higher than those reported for full-length KaiA and KaiC binding for *S. elongatus* (2.5 μM) (33) and *T. elongatus* (1.3 μM) (32). We think that these discrepancies arise from (*i*) the higher local concentration of KaiC$^{AL+tail}$ segments on a KaiC hexamer, and (*ii*) the possibility that the KaiA-KaiC interaction is more extensive than that observed in the NMR structure (Fig. 1*A*).

KaiA^N Attenuates the KaiA–KaiC Interaction and Is Important for KaiB Function. The N-terminal domain of KaiA, KaiA^N (residues 1–135), did not have any detectable affinity for KaiC$^{AL+tail}$, as gauged by fluorescence anisotropy experiments (Fig. 4*A*, ◇). In addition, KaiA^N has no effect on the phosphorylation activity of KaiC (blue ▲, Fig. 2*B*) (10). Thus, the KaiA–KaiC interaction probably involves only weak, if any, interactions between KaiA^N and KaiC. However, full-length KaiA had a weaker affinity for KaiC$^{AL+tail}$ and enhanced KaiC autophosphorylation less than KaiA^C (Fig. 4*A*, △ and □; Fig. 2*B*, pink ● and orange ♦). KaiA^N may attenuate the KaiA–KaiC interaction by affecting the structure of KaiA^C (29).

Apparently, KaiB inactivates KaiA in a complex with pST-KaiC, which allows the ensemble of KaiC proteins to autodephosphorylate (23, 24). We found that KaiA^N was important for this KaiB function. As shown in Fig. 2*C* (orange ♦), KaiB had little effect on KaiA^C-induced KaiC autophosphorylation. The observation that *S. elongatus* clones that express KaiA^C instead of KaiA generate very weak 40-h rhythms (34) may be attributable to the inability of KaiB to inactivate KaiA^C in a complex with pST-KaiC.

KaiB Does Not Interact with the A-Loop. It has been shown that the kinetic ordering of phosphorylation at S431 and T432 for an ensemble of KaiC proteins in the presence of KaiA and KaiB is as follows (23, 24): ST → SpT → pSpT → pST → ST. Apparently, the oscillation depends on the fast buildup of pSpT-KaiC under stimulation by KaiA, followed by the slow inactivation of KaiA on pST-KaiC by KaiB (24). How KaiB achieves this inactivation is unclear. Does KaiB interact directly with the A-loop? Fluorescence anisotropic experiments did not detect any binding between KaiB and KaiC$^{AL+tail}$ in either *S. elongatus* (Fig. 4*A*, ○) or *T. elongatus* (Fig. 4*B*, ○). Furthermore, KaiB by itself does not affect the phosphorylation of KaiC (Fig. 2*D*) (17, 18, 24). Thus, KaiB likely affects the dynamic equilibrium of the A-loop indirectly by hindering its interaction with KaiA.

A-Loop Displacement Probably Moves ATP Closer to the Sites of Phosphorylation. To the best of our knowledge, the longest distance reported between the γ-phosphate group of ATP and an acceptor oxygen (serine hydroxyl group) is 5.3 Å in bovine cAMP-dependent protein kinase (35), which has since been suggested to be an overestimate (36). In the crystal structure of KaiC, the A-loops are buried, and the γ-phosphate group of ATP is 8.5 and 6.6 Å from the hydroxyl oxygens of S431 and T432, respectively (Fig. 5), which explains why KaiC by itself had a low level of autokinase activity (Fig. 2*A*, pink ●). It is, therefore, probable that A-loop exposure significantly repositions ATP closer to the sites of phosphorylation.

Putative interactions between the adenine base and residues I472 and D474, as inferred from the structure of KaiC (15), may help prevent ATP from approaching the sites of phosphorylation when A-loops are buried (Fig. 5*A*). A D474A substitution

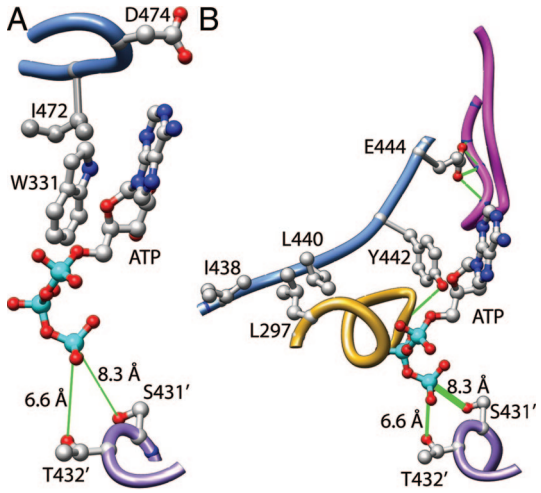

Fig. 5. Putative interactions between ATP and KaiC, as inferred from the x-ray crystal structure (15). Atoms are shown in ball and stick form (gray, carbon; red, oxygen; blue, nitrogen; cyan, phosphorus). The prime (′) is used to denote residues from an adjacent subunit. Green lines indicate potential hydrogen bonds and the distances between the γ-phosphorus atom of ATP and the hydroxyl oxygens of S431′ and T432′. (*A*) The structure of KaiC suggests that the position of ATP depends in part on interactions with I472, D474, and W331. (*B*) The position of the γ-phosphorus atom of ATP may be coupled to the interaction between E444 and the A-loop by way of the P-loop. The side chains of residues that may be part of this coupling are shown.

attenuated the effect of KaiA and KaiB on KaiC phosphorylation kinetics (Fig. S4, black ▲). The variant I472A (Fig. S4, blue ■), however, was constitutively hyperphosphorylated, suggesting that ATP could more closely approach T432 and S431. We think that exposure of A-loops weakens the interaction between I472 and ATP. The ATP seems to also be stabilized by W331 because a W331A substitution also created a constitutively hyperphosphorylated KaiC variant (Fig. S4, green ♦).

E444 apparently forms hydrogen bonds with A-loop residues and is part of a short segment (residues 438–444; blue ribbon, Fig. 5*B*) that seems to interact with residues at or adjacent to the P-loop of the CII domain (residues 288–295; gold ribbon, Fig. 5*B*). We anticipate that this chain of interactions couples the A-loop and γ-phosphate positions. A-loop exposure may disrupt its interaction with E444, causing the 438–444 segment to shift and thereby adjust the position of the P-loop, which, in turn, would move the γ-phosphate closer to the hydroxyl groups of T432 and S431. As a test of this hypothesis, we introduced an E444D substitution to disrupt the interactions with the A-loop. We found that this KaiC variant was constitutively hyperphosphorylated at ≈100% in the presence or absence of KaiA and KaiB (Fig. S4, black ●). L297A and L440A substitutions, which would be a good test of the proposed coupling between the A-loop and ATP position, yielded insoluble KaiC variants.

Discussion

The A-loop Is the Master Switch That Determines KaiC Activities. KaiC is both an autokinase and an autophosphatase. The balance between these two activities is modulated by phosphoform-dependent interactions between KaiC and KaiA and KaiB, and by the phosphoforms themselves, irrespective of KaiA and KaiB (23, 24). Here, we propose how KaiA and KaiB manipulate KaiC activity: the A-loop is the master switch and its dynamic equilibrium between buried and exposed states determines the levels of autokinase and autophosphatase activities (Fig. 6); KaiA directly binds to and stabilizes the exposed state of the A-loop. KaiB does not directly interact with the A-loop; we predict that KaiB stabilizes the buried state of the A-loop indirectly by

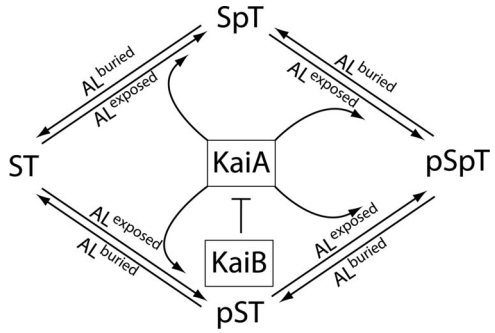

Fig. 6. A-loop model. The steady-state level of phosphorylation of KaiC is determined by the dynamic equilibrium of the A-loops (AL). If the buried state of the A-loops (AL^{buried}) is favored, then the steady-state phosphorylation level of KaiC is lowered; if the exposed state of the A-loops ($AL^{exposed}$) is favored, the steady-state phosphorylation level is increased. KaiA stabilizes $AL^{exposed}$, whereas KaiB prevents KaiA from doing so by immobilizing it on the pST-KaiC phosphoform.

hindering its interaction with KaiA. Indeed, existing data suggest that KaiB does not affect KaiC activity directly but, rather, blocks KaiA stimulation of KaiC activity (Fig. 2*C*, pink ●) (17, 18, 24).

A-Loop Burial/Exposure May Be Cooperative. Each buried A-loop in the KaiC hexamer appears to make several hydrogen bonds with the adjacent A-loops (Fig. S3). The implication is that exposure of one A-loop destabilizes the buried states of the adjacent ones and raises the possibility that the burial and exposure of A-loops are cooperative processes. However, the rate of ST-KaiC → SpT-KaiC has a hyperbolic, rather than sigmoidal, dependence on KaiA concentration (24), which argues against cooperativity. We suggest that when a single KaiA binds to a KaiC hexamer (30, 32), it stabilizes the exposed state of the two A-loops to which it binds (Fig. 1*A*), shifting the dynamic equilibrium of the four remaining A-loops toward the exposed state. This scenario could produce the hyperbolic dependence for ST-KaiC → SpT-KaiC, as demonstrated by Rust *et al.* (24).

KaiB Inactivates KaiA by Hindering Its Interaction with A-Loops. Our data suggest that KaiB induces KaiC autodephosphorylation by hindering the interaction between KaiA and A-loops. There are two possible ways by which KaiB inactivates KaiA: either KaiB interacts directly with KaiA and thereby immobilizes it on pST-KaiC or the KaiB–pST-KaiC interaction affects the pST-KaiC–KaiA interaction, such that KaiA is trapped by pST-KaiC. Our observation that $KaiA^{C}$-induced KaiC autophosphorylation was immune to KaiB suggests that $KaiA^{N}$ is necessary for KaiB activity. Whether the KaiA–KaiB interaction is direct or indirect is still unclear.

Downstream Effects of A-Loop Exposure. The ATP bound in the CII domain is too far from S431 and T432 for phosphoryl transfer (Fig. 5) and explains why KaiC by itself had a greater autophosphatase than autokinase activity (Fig. 2*A*, pink ●). Our data suggest that I472 helps prevent ATP from approaching the sites of phosphorylation (Fig. S4), probably through direct interactions with ATP. A-loop exposure likely repositions the ATP closer to the sites of phosphorylation through weakening the I472–ATP interaction, and disrupting the E444–A-loop interaction, thereby shifting the P-loop.

Differences Between *in Vitro* and *in Vivo* Oscillations. The dominant negative effects of KaiC487 and KaiC497 expression in a WT background suggest that these KaiC variants, which are unable to restore rhythmicity to a *kaiC*-null strain, either participate in hexamer formation with WT KaiC monomers, rendering them nonfunctional, or compete with WT subunits for interaction with the circadian output pathways. The former possibility, supported experimentally in Fig. S7, contrasts with *in vitro* data in which oscillation of WT KaiC phosphorylation is unaffected by addition of nonshuffling KaiC variants (27). These data suggest that nascent proteins form mixed hexamers when both WT and mutant KaiC variants are coexpressed in the cell, such that protein dynamics of synthesis and degradation may play important roles *in vivo* that are not required for the basic oscillation *in vitro*.

Materials and Methods

Sample Preparation. ***KaiA and KaiB.*** The genes encoding KaiA and KaiB from *S. elongatus* and *T. elongatus* were cloned into the pET32a+ vector (Novagen) between BamHI and NcoI sites, the resulting plasmids were used to transform *Escherichia coli* BL21(DE3), and sequences were confirmed (Gene Technologies Laboratory, Texas A&M University) (see Table S1). Transformed *E. coli* cultures in log phase in LB at 37°C were induced to overexpress recombinant KaiA or KaiB with 1 mM isopropyl β-D-thiogalactopyranoside (Calbiochem). Cells were harvested after 6 h, and pellets were resuspended in 50 mM NaCl, 20 mM Tris·HCl, pH 7.0. Cell suspensions were passed twice through a chilled French press cell, and lysates were clarified by centrifugation at 20,000 × *g* for 60 min at 4°C. Tagged proteins were isolated on a Ni-charged chelating column. Proteases and ATPases were removed by anion-exchange chromatography (buffer A: 20 mM NaCl, 20 mM Tris·HCl, pH7; buffer B: 1 M NaCl, 20 mM Tris·HCl, pH 7; gradient: 0–80% buffer B over 16 5-mL column volumes). Further details are provided in *SI Text*.

KaiC. Genes encoding KaiC from *S. elongatus* and *T. elongatus* were cloned into the pGEX-6P-2 vector (GE Healthcare) between BamHI and XhoI sites, and the resulting plasmids were used to transform *E. coli* DH5α, which produced more soluble recombinant KaiC than did *E. coli* BL21(DE3). KaiC truncation variants KaiC487, KaiC494, KaiC495, KaiC496, and KaiC497 were constructed by inserting stop codons to terminate translation after residues 487, 494, 495, 496, and 497, respectively, using the QuikChange method from Stratagene. Protein purification, analysis, and storage were similar as for KaiA and KaiB and are described in *SI Text*.

KaiC Phosphorylation Kinetics. Phosphorylation assays in sterile 1-ml tubes in a 30°C water bath included KaiA and KaiB at 1.5 μM and 4.5 μM final concentrations in the autophosphorylation assay buffer. A "time zero" sample was taken immediately after KaiC (3.4 μM) was added. Periodically, 38-μl aliquots were removed and denatured at 60°C for 15 min with 6 μl of SDS/PAGE gel-loading dye (100 mM Tris·HCl at pH 6.8 with 4% SDS, 0.2% bromophenol blue, 20% glycerol, and 400 mM β-mercaptoethanol). A sample (10 μl) of each was loaded onto 9 × 10 cm SDS polyacrylamide gels (4% stacking, 6.5% running) with 15 wells (10 × 3 × 0.75 mm). Further details are given in *SI Text*.

Fluorescence Anisotropy Experiments. Preparation of the $KaiC^{AL+tail}$ peptide labeled with fluorescein is given in *SI Text*. Fluorescence anisotropy experiments on the fluorescein-labeled $KaiC^{AL+tail}$ peptide were carried out with a PC1 photon counting spectrofluorometer (ISS) with a sample temperature of 25°C. The excitation wavelength was set to 487 nm, and orthogonal emission intensities, $I_{\parallel}$ and $I_{\perp}$, were measured at 523 nm; fluorescence anisotropy, r, was determined using the equation: $r = (I_{\parallel} - I_{\perp})/(I_{\parallel} + I_{\perp})$. The $KaiC^{AL+tail}$ peptide concentration in an initial volume of 1.8 ml was 100 nM. Fluorescence anisotropies were measured as a function of the concentrations of KaiA, KaiA variants, and KaiB. Dissociation constants were calculated by fitting anisotropic data using DYNAFIT (37) with a simple 1:1 binding model.

Cyanobacterial Strains, Culture Conditions, and Bioluminescence Assays. WT *S. elongatus* PCC 7942 and its derivatives were propagated in BG-11 medium with appropriate antibiotics at 30°C, as described previously (38, 39). Ectopic alleles of various KaiC constructs, described in Tables S2 and S3, were introduced into neutral site I of the *S. elongatus* chromosome (38, 39). Bioluminescence assays of these strains were performed on a Packard TopCount scintillation counter (PerkinElmer Life Sciences) according to a previous protocol (39).

ACKNOWLEDGMENTS. We thank Elizabeth Ihms and Larry Dangott of the Texas A&M Protein Chemistry Laboratory for technical assistance and David Giedroc and Gregory Reinhart for assistance with their fluorometers. This work was supported by grants from the National Institutes of Health (GM064576 to A.L.; GM62419 and NS39546 to S.S.G.), Advanced Research Program Project 000517-0003-2006 (to A.L.), and University of California at Merced startup funds (to A.L.).

1. Dunlap JC, Loros JJ, DeCoursey PJ (2004) *Chronobiology: Biological Timekeeping* (Sinauer, Sunderland, MA).
2. Bell-Pedersen D, *et al.* (2005) Circadian rhythms from multiple oscillators: Lessons from diverse organisms. *Nat Rev Genet* 6:544–556.
3. Kondo T, *et al.* (1993) Circadian rhythms in prokaryotes: Luciferase as a reporter of circadian gene expression in cyanobacteria. *Proc Natl Acad Sci USA* 90:5672–5676.
4. Ditty JL, Williams SB, Golden SS (2003) A cyanobacterial circadian timing mechanism. *Annu Rev Genet* 37:513–543.
5. Woelfle MA, Ouyang Y, Phanvijhitsiri K, Johnson CH (2004) The adaptive value of circadian clocks: An experimental assessment in cyanobacteria. *Curr Biol* 14:1481–1486.
6. Ouyang Y, Andersson CR, Kondo T, Golden SS, Johnson CH (1998) Resonating circadian clocks enhance fitness in cyanobacteria. *Proc Natl Acad Sci USA* 95:8660–8664.
7. Liu Y, *et al.* (1995) Circadian orchestration of gene expression in cyanobacteria. *Genes Dev* 9:1469–1478.
8. Nakahira Y, *et al.* (2004) Global gene repression by KaiC as a master process of prokaryotic circadian system. *Proc Natl Acad Sci USA* 101:881–885.
9. Ishiura M, *et al.* (1998) Expression of a gene cluster. *kaiABC* as a circadian feedback process in cyanobacteria. *Science* 281:1519–1523.
10. Williams SB, Vakonakis I, Golden SS, LiWang AC (2002) Structure and function from the circadian clock protein KaiA of Synechococcus elongatus: A potential clock input mechanism. *Proc Natl Acad Sci USA* 99:15357–15362.
11. Vakonakis I, *et al.* (2004) NMR structure of the KaiC-interacting C-terminal domain of KaiA, a circadian clock protein: Implications for the KaiA-KaiC interaction. *Proc Natl Acad Sci USA* 101:1479–1484.
12. Ye S, Vakonakis I, Ioerger TR, LiWang AC, Sacchettini JC (2004) Crystal structure of circadian clock protein KaiA from Synechococcus elongatus. *J Biol Chem* 279:20511–20518.
13. Garces RG, Wu N, Gillon W, Pai EF (2004) Anabaena circadian clock proteins KaiA and KaiB reveal a potential common binding site to their partner KaiC. *EMBO J* 23:1688–1698.
14. Hitomi K, Oyama T, Han S, Arvai AS, Getzoff ED (2005) Tetrameric architecture of the circadian clock protein KaiB: A novel interface for intermolecular interactions and its impact on the circadian rhythm. *J Biol Chem* 280:19127–19135.
15. Pattanayek R, *et al.* (2004) Visualizing a circadian clock protein: Crystal structure of KaiC and functional insights. *Mol Cell* 15:375–388.
16. Nakajima M, *et al.* (2005) Reconstitution of circadian oscillation of cyanobacterial KaiC phosphorylation in vitro. *Science* 308:414–415.
17. Xu Y, Mori T, Johnson CH (2003) Cyanobacterial circadian clockwork: Roles of KaiA, KaiB and the kaiBC promoter in regulating KaiC. *EMBO J* 22:2117–2126.
18. Kitayama Y, Iwasaki H, Nishiwaki T, Kondo T (2003) KaiB functions as an attenuator of KaiC phosphorylation in the cyanobacterial circadian clock system. *EMBO J* 22:2127–2134.
19. Iwasaki H, Nishiwaki T, Kitayama Y, Nakajima M, Kondo T (2002) KaiA-stimulated KaiC phosphorylation in circadian timing loops in cyanobacteria. *Proc Natl Acad Sci USA* 99:15788–15793.
20. Tomita J, Nakajima M, Kondo T, Iwasaki H (2005) No transcription-translation feedback in circadian rhythm of KaiC phosphorylation. *Science* 307:251–254.
21. Xu Y, *et al.* (2004) Identification of key phosphorylation sites in the circadian clock protein KaiC by crystallographic and mutagenetic analyses. *Proc Natl Acad Sci USA* 101:13933–13938.
22. Nishiwaki T, *et al.* (2004) Role of KaiC phosphorylation in the circadian clock system of Synechococcus elongatus PCC 7942. *Proc Natl Acad Sci USA* 101:13927–13932.
23. Nishiwaki T, *et al.* (2007) A sequential program of dual phosphorylation of KaiC as a basis for circadian rhythm in cyanobacteria. *EMBO J* 26:4029–4037.
24. Rust MJ, Markson JS, Lane WS, Fisher DS, O'Shea EK (2007) Ordered phosphorylation governs oscillation of a three-protein circadian clock. *Science* 318:809–812.
25. Mori T, *et al.* (2007) Elucidating the ticking of an in vitro circadian clockwork. *PLoS Biol* 5:841–853.
26. Emberly E, Wingreen NS (2006) Hourglass model for a protein-based circadian oscillator. *Phys Rev Lett* 96:038301–038304.
27. Ito H, *et al.* (2007) Autonomous synchronization of the circadian KaiC phosphorylation rhythm. *Nat Struct Mol Biol* 14:1084–1088.
28. Kitayama Y, Nishiwaki T, Terauchi K, Kondo T (2008) Dual KaiC-based oscillations constitute the circadian system of cyanobacteria. *Genes Dev* 22:1513–1521.
29. Vakonakis I, LiWang AC (2004) Structure of the C-terminal domain of the clock protein KaiA in complex with a KaiC-derived peptide: Implications for KaiC regulation. *Proc Natl Acad Sci USA* 101:10925–10930.
30. Pattanayek R, *et al.* (2006) Analysis of KaiA-KaiC protein interactions in the cyanobacterial circadian clock using hybrid structural methods. *EMBO J* 25:2017–2028.
31. Akiyama S, Nohara A, Ito K, Maeda Y (2008) Assembly and disassembly dynamics of the cyanobacterial periodosome. *Mol Cell* 29:1–14.
32. Hayashi F, *et al.* (2004) Stoichiometric interactions between cyanobacterial clock proteins KaiA and KaiC. *Biochem Biophys Res Commun* 316:195–202.
33. Kageyama H, *et al.* (2006) Cyanobacterial circadian pacemaker: Kai protein complex dynamics in the KaiC phosphorylation cycle in vitro. *Mol Cell* 23:161–171.
34. Uzumaki T, *et al.* (2004) Crystal structure of the C-terminal clock-oscillator domain of the cyanobacterial KaiA protein. *Nat Struct Mol Biol* 11:623–631.
35. Granot J, Mildvan AS, Bramson HN, Kaiser ET (1980) Magnetic resonance measurements of intersubstrate distances at the active site of protein kinase using substitution-inert cobalt(III) and chromium(III) complexes of adenosine 5′-(β,γ-methylenetriphosphate). *Biochemistry* 19:3537–3543.
36. Mildvan AS (1997) Mechanisms of signaling and related enzymes. *Proteins Struct Funct Genet* 29:401–416.
37. Kuzmic P (1996) Program DYNAFIT for the analysis of enzyme kinetic data: Application to HIV proteinase. *Anal Biochem* 237:260–273.
38. Clerico EM, Ditty JL, Golden SS (2007) Specialized techniques for site-directed mutagenesis in cyanobacteria. In *Methods in Molecular Biology*, ed Rosato E (Humana Press, Totowa), 362:155–172.
39. Mackey SR, Ditty JL, Clerico EM, Golden SS (2007) Detection of rhythmic bioluminescence from luciferase reporters in cyanobacteria. In *Methods in Molecular Biology*, ed Rosato E (Humana Press, Totowa), 362:115–130.
40. Pettersen EF, *et al.* (2004) UCSF Chimera - A visualization system for exploratory research and analysis. *J Comput Chem* 25:1605–1612.
41. Ivleva NB, Golden SS (2007) Protein extraction, fractionation, and purification from cyanobacteria. In *Methods in Molecular Biology*, ed Rosato E (Humana Press, Totowa), 362:365–373.
42. Ditty JL, Canales SR, Anderson BE, Williams SB, Golden SS (2005) Stability of the Synechococcus elongatus PCC 7942 circadian clock under directed anti-phase expression of the kai genes. *Microbiology* 151:2605–2613.